EVALUATION OF MECHANICAL AND THERMAL FATIGUE PROPERTIES OF ALUMINA CERAMICS

Manabu Takatsu and Tadahiro Nishikawa

Dept. Materials Science and Engineering
Nagoya Institute of Technology
Gokiso-cho, Showa-ku, Nagoya 466, Japan

ABSTRACT

It is well known that ceramics generally exhibit incompatible properties. For alumina ceramics having the same porosity, the critical stress intensity factor K_{IC} and bending strength S_f are variable in inverse proportion with the amount of impurity or particle size etc. Therefore, it is important to consider their mechanical properties for utilizing alumina ceramics The authors investigated the mechanical or thermal fatigue properties of several ceramics, and arranged the data with fracture mechanic technique. The fundamental properties on the fracture mechanics were related to the fracture behavior, in which the inter-granular fracture was predominant for alumina ceramics. The acceleration to short life was observed on mechanical cyclic fatigue test, comparing with static fatihue test. However, since the stress ratio could not be varied on thermal fatigue test, one fatigue parameter n hardly changed. Other fatigue parameter A clearly changed in correspondence with its microstructure. The n values on thermal fatigue test were nearly equal to those on mechanical fatigue test. The feedback treatment to control and obtain the most suitable microstructure for structural material, was investigated and discussed.

INTRODUCTION

Ceramics generally exhibit incompatible properties, so it is difficult to obtain materials having large bending strength and large critical stress intensity factor simultaneously. Under conditions in use, it may be sufficient to increase only one of the two values. Mechanical and thermal fatigue properties do not always correspond to the intrinsic mechanical properties, such as bending strength and frac-

ture toughness. For example, some investigators have reported that materials exhibiting a rising R curve behavior are difficult to use under cyclic load at small stress ratio R, but thses fatigue properties could not be trested quantitatively

In this paper, the mechanical and thermal properties of some kinds of alumina ceramics were investigated, in order to control their microstructure and apply them to structural materials.

MATERIALS AND TESTING METHOD

Materials

Test pieces used in the experiments were four kinds of commercial alumina ceramics and one synthesized ceramics from high purity alumina powder, which was sintered at 1450℃ for 30 min. For the fatigue test, the 3x4x40 mm specimens were lapped to mirror finish with ground corners. The mechanical and thermal properties of alumina ceramics were listed in Table 1. Fig. 1 shows the relation between the flexural strength S_f and fracture toughness K_{IC}. Hardness was measured by Vickers indentation and elastic modulus was measured by an ultrasonic pulse method. Flexural strengths were measured by a three-point bending test to determine the Weibull parameter. The K_{IC} value was determined by the IF method, and bulk density by the Archimedes method.

Table 1 Mechanical and thermal properties of alumina ceramics

Test piece	Purity wt%	Density g/cm³	Flexual strength MPa	Weibull's modulus -	Fracture toughness MPam$^{0.5}$	Young's modulus GPa	Poisson's ratio -	Thermal expansion coefficient x10^{-6} /K	Thermal conductivity W/mK	Specific heat J/kg K
A	92.0	3.49	325	13.3	2.7	—	—	—	—	—
B	97.0	3.69	317	10.9	2.6	350	0.23	7.70	21	840
C	99.0	3.93	375	16.2	3.7	360	0.24	7.70	29	840
D	99.5	3.93	413	18.8	2.9	402	0.25	7.75	27	840
E	99.99	3.96	474	6.5	2.7	400	0.25	7.80	29	840

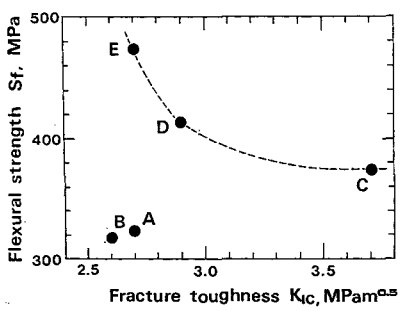

Fig. 1 Fracture toghness and flexural strength results for alumina ceramics

Mechanical Fatigue Test [1]

Cyclic and static fatigue tests were performed under maximum applied stress σ_{max}, which was 70 to 100% of mean bending strength, to measure the time to failure t_f. Cyclic fatigue test was conducted on a high frequency cyclic instrument, which provides a sinusoidal cyclic frequency of approximately 550 Hz with a stress ratio ($R=\sigma_{min}/\sigma_{max}$) of 1.0 or 0.1 and one-side oscillation. The experiment was conducted at room temperature under 50% R.H. for a maximum of 10^5 seconds.

Thermal Fatigue Test [2]

Test pieces pre-cracked by Knoop indentation were heated in a constant temperature, and quenched in water. Their propagated crack lengths were then measured. Heat transmission condition varied from natural convection to nucleant boiling in the range of this experimental temperature. Therefore, we previously corrected the heat transfer coefficient and illustrated the ($K_{I\,max}/K_{IC}$)-V curve. Subsequently, the thermal fatigue behavior of each alumina ceramics was discussed quantitatively using fatigue parameter n and A.

RESULTS AND DISCUSSIONS

I Feedback from Cyclic Fatigue Data

If the cyclic fatigue property is dependent on the cyclic number, the experiment must be performed at low frequency and requires much time to feedback the data for development of material. The fatigue test in the present study carried out at high frequency, which was above 250 Hz. At these high frequencies, it is known that fatigue properties are merely dependent on stress amplitude. Fatigue data were collected and control of the microstructure for alumina ceramics was discussed.

a) Arrangement of Fatigue Data [3]

Fatigue data were arranged by the following method. The velocity of the crack propagation in the region under the critical stress intensity factor (K_{IC}) is represented by the empirical formula:

$$V=(dc/dt)=A(K_I/K_{IC})^n \qquad (1)$$

where, V is crack propagation velocity, c is crack length for time t, K_I is stress intensity factor and A,n are constants.

Assuming a randomly picked sample with an initial crack length C_i, which requires a time to failure t_f until it grows to length C_f and begins to have an unstable growth, the following equation is obtained by integrating Eq. (1):

$$S^{n-2}=[(n-2)/2](A/K_{IC}^2)Y^2\int_0^{t_f}[\sigma(t)]^n dt \qquad (2)$$

In this equation, S denotes the strength when a dynamic load has been exerted on a

sample possessing an initial crack length C_i, and has a relation: $S=K_{IC}/(YC_i^{1/2})$. The relationship of S with the bending strength S_f at a loading stress velocity σ is obtained as follows by solving Eq. (1) under the condition of $\sigma(t)=\sigma t$:

$$S^{n-2}=[(n-2)/2(n+1)](A/K_{IC}^2)Y^2\sigma^{-1}S_f^{n+1} \quad (3)$$

By substituting Eq. (3) in Eq. (2) and rearranging, the following is obtained:

$$[\sigma^{-1}/(n+1)]S_f^{n+1}=\int_0^{t_f}\{\sigma(t)\}^n dt \quad (4)$$

By carrying out the integration on the right side of Eq. (4) with the time range of $(t_2>t>t_1)$ that satisfies the stress $(\sigma(t)>\sigma_{lim})$ corresponding to the range $(K_I>K_{Ilim})$ where Eq. (1) is applicable, and by making the stress term of Eq. (4) non-dimensional using the applied stress σ_{max} and then rearranging, Eq. (5) is obtained.

$$\log(\sigma_{max}/S_f)=[-1/(n+1)]\log(t_f\cdot g^{-1})-\log B \quad (5)$$

where g^{-1} is the term relative to the applied stress wave-form given by Eq.(6).

$$g^{-1}=\int_{t_1}^{t_2}\{\sigma(t)/\sigma_{max}\}^n/\lambda\, dt \quad (6)$$

According to Eq. (5) and from all the fatigue test data obtained, S_f and g^{-1} could be calculated; then by plotting logarithmic graphs of two expressions σ_{max}/S_f and $t_f\cdot g^{-1}$, the fatigue parameter n could be calculated.

b) Inducement of Fatigue Parameters in Relation to Microstructure [4]

Parameter n can be calculated from the slope of the line in eq. (5) at a given stress ratio for each alumina. Another fatigue parameter A exhibits generally a good correlation with parameter n. Minnear et al. [5] found that two parameters have a linear relationship at semi-logarithmic graph. The authors confirmed that a different fatigue behavior occurred at each given stress ratio. Therefore, we pointed out that the change of parameter A in figure was concealed by the large exponent part of A. To introduce parameter A, the ratio $\Delta A=A_C/A_S$ was used where the A value representing static fatigue was denoted as A_S, and the A value representing the cyclic fatigue by A_C. Eq. (2) was solved with the value A, resulting in Eq. (7):

$$A=[2/(n-2)](K_{IC}^2/Y^2\cdot\sigma_{max}^2\cdot t_f\cdot g^{-1})(S/\sigma_{max})^{n-2} \quad (7)$$

With A_S and A_C denoting static fatigue for A and cyclic fatigue for A, respectively, to obtain ΔA. The logarithmic expression is found in Eq. (8).

$$\log\Delta A=\log\{t_f\}_S-\log\{t_f\cdot g^{-1}\}_C+A' \quad (8)$$

where,

$$A'=\log[(n_S-2)/(n_C-2)]+(n_S-n_C)\log(\sigma_{max}/S) \quad (9)$$

In the case of static fatigue, g=1. If it is assumed that approximately $S=S_f$, Eq. (8) represents the distance in the direction of the horizontal axis, between the approximated linear cyclic fatigue and the approximated linear static fatigue at

$\sigma_{max}/S_f=1.0$, plotted on a graph of $\log(\sigma_{max}/S_f)$ and $\log(t_f \cdot g^{-1})$.

The fatigue data were classified in terms of stress ratio R, and shown in Fig. 2 [4] . For the materials having $n_s = n_c$, A' value in eq. (8) became constant and the fatigue mechanism did not change with applied stress. This tendency was observed for materials with relatively small bending strength, whereas for $n_s \neq n_c$, the fatigue mechanism depended on the applied stress. If material exhibited $n_s > n_c$, materials under cyclic fatigue had essentially a short life in the lower stress region. If the material exhibited $n_s < n_c$, material had a long life in the lower stress region. This suggested that a lower limit value for crack propagation might exist.

The fatigue behavior was discussed using parameter A. The $\log \Delta A$ was taken with R. The $\log \Delta A$ indicated the distance in the horizontal shift from the static fatigue data at $\sigma_{max}/S_f=1.0$. Its positive value means the acceleration to short life time and negative means the deceleration. These treatments clarified the degree of acceleration under cyclic load quantitatively with decreasing R. Especially, this parameter was sensitive to the microstructure of ceramics using a densification additive.

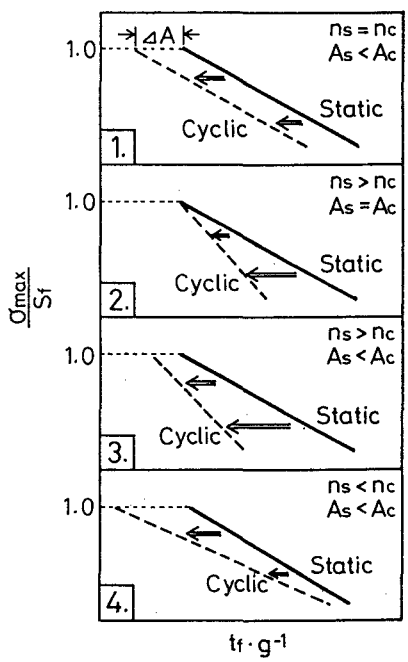

Fig. 2 Schematic diagrams and classification of n and A as the parameters of cyclic fatigue behavior

c) Fatigue data of Alumina Ceramics

Static and cyclic fatigue results of each test piece were shown in Fig. 3, in terms of the relation between the maximum applied stress σ_{max} and the time to failure t_f. Data on three-point bending strength are shown on the left side in Fig. 3 as an average value with deviation. In order to express the above fatigue behavior quantitatively, the data were normalized using the above Eq. (4). The normalized results were shown in Fig. 4. Static fatigue test results were indicated by the solid line and the range of standard deviation by the dashed line, as obtained by the least squares method. If experimental data under cyclic

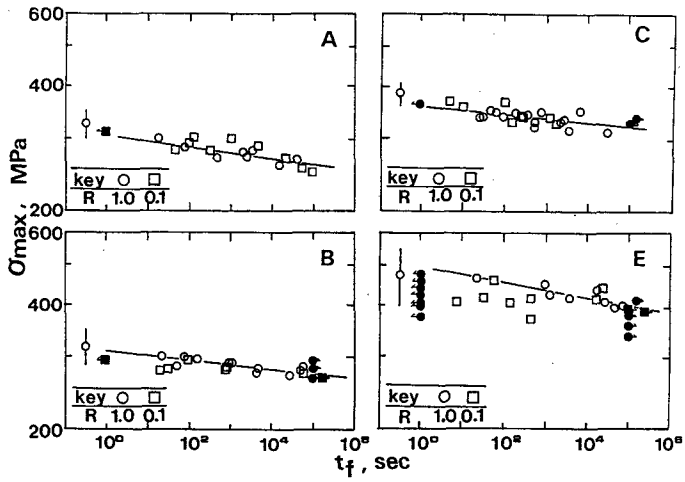

Fig. 3 Relations between maximum loading stress σ_{max} and fatigue life t_f for alumina ceramics under the different stress ratio R

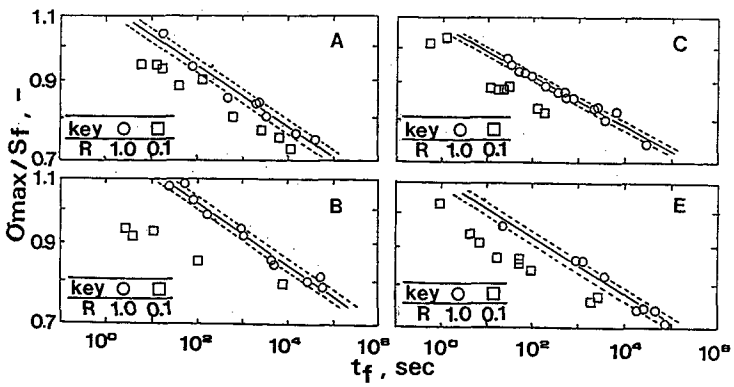

Fig. 4 Analysisi of cyclic fatigue properties of alumina ceramics by estimated method based on empirical equation of subcritical crack growth

load were located between the two dashed lines, the crack propagation rate under cyclic load did not change with that under static load. Cyclic fatigue data for any alumina ceramics shifted toward the short life side. This suggested that the crack propagation rate was accelerated under cyclic fatigue test. The degree and tendency of acceleration were slightly different for alumina ceramics, and indicated by fatigue parameters and shown in Fig. 5. Generally, chipping is frequently observed for materials, in which the trans-granular fracture was predominant. By decreasing the stress ratio, the crack propagation velocity is accelerated. Therefore, it is considered that minus correlation was observed between the crack propagation velocity and fracture toughness [6] .

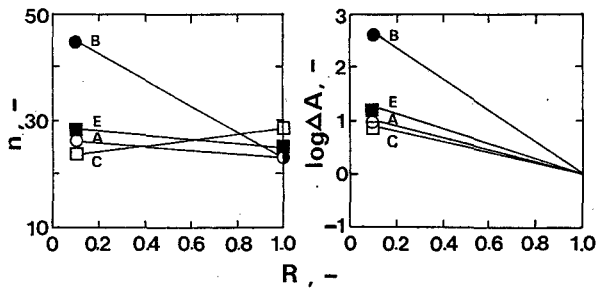

Fig. 5 Relations between stress ratio R and fatigue parameter n (left) or log Δ A(right)

II FeedBack from thermal Fatigue Data

Kamiya et al. [7] performed the thermal fatigue test by the water quenching method, using non pre-cracked test piece. The data were normalized the following equation derived from K_I-V curve.

$$N/N' = (\Delta T_{N'}/\Delta T_N)^n \quad (10)$$

where N and N' are the critical cyclic number for temperature difference ΔT_N and $\Delta T_{N'}$, respectively, n is a material constant.

The authors applied the one-dimensional thermal shock and investigated the crack propagation behavior, using pre-cracked test piece with a straight notch [8] .

a) Arrangement of Fatigue Data [2]

Firstly, calculation of K_I was tried, considering the pre-crack length of the test piece after quenching. K_I-V curve was empirically indicated as Eq. (1), which can be rewritten to incorporate the transitional thermal stress.

$$V = \Delta c/\Delta t_s = A(K_{I\,max}/K_{IC})^n \quad (11)$$

$$\Delta t_s = \Delta t_T \cdot g \quad (12)$$

$$g = (1/\Delta t_T) \int_{t_1}^{t_2} [K_I/K_{I\,max}]^n dt \qquad (13)$$

where Δc is the propagated crack length after quenching and Δt_s is assumed time for applying constant thermal stress $K_{I\,max}$. Meanwhile, K_I in Eq. (13) is obtained from Erdogan equation, in which the one-side opening crack was assumed.

$$K_I^* = (2/\pi e) \int_0^e \sigma^*(\xi_1)\sqrt{\xi_1(e-\xi_1)}\, d\xi_1 \qquad (14)$$

b) Thermal Fatigue Data of Alumina Ceramics

The changes of observed crack length subjected to cyclic water quenching was shown in Fig. 6. ($K_{I\,max}/K_{IC}$)-V curves of alumina ceramics obtained was shown in Fig. 7. Compared with alumina ceramics having the same porosity, bending strength and fracture toughness are variable in inverse proportion, shown in Fig. 1. For the thermal fatigue behavior of alumina, in which inter-granular fracture was mainly observed, the n values were constant but the logA values decreased with increasing particle size. This indicated that the crack propagation rate became low. For those in which more larger particles or pores were observed, the log A values and crack propagation rate also differed. These different behaviors upon thermal fatigue may be explained by the propagation mechanism on crack tips. In general, the control of microstructure for thermally used ceramics is important, for determining the crack propagation pass.

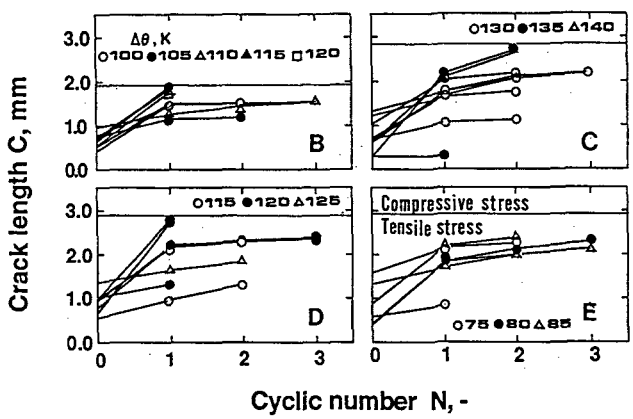

Fig. 6 Changes of observed crack growth subjected to cyclic water quenching

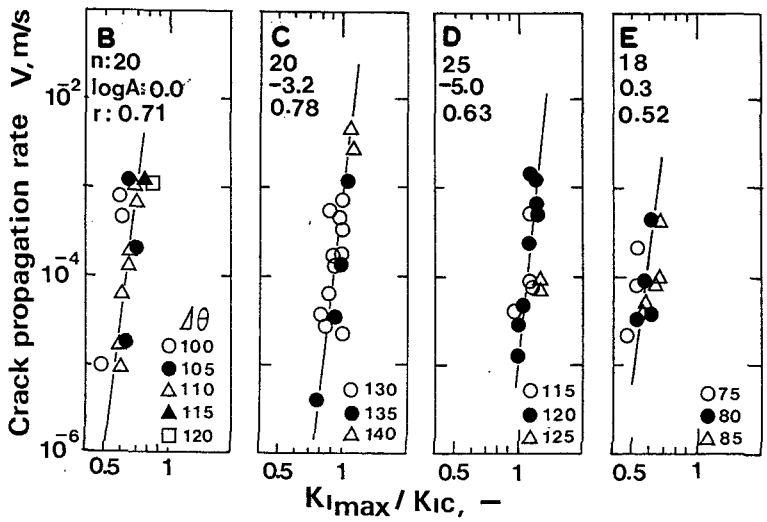

Fig. 7 ($K_{I\,Max}/K_{IC}$)-V curves of alumina ceramics obtained by cyclic water quenching method

III Fatigue Mechanism

Many investigators have proposed theories about the fatigue mechanism for ceramics. Generally, the possible crack-advance mechanism during cyclic fatigue test were classified into two groups, which were intrinsic and extrinsic mentioned by Ritchie [9] . Considering with fractography of alumina ceramics, in which the inter-granular fracture was predominant, incomplete crack-closure or wedging of debris might cause the acceleration on the fatigue test.

Ceramics does not exhibit plasticity but has large elastic modulus, compared with metallic material. Especially, ceramics can not relax the generated strain and causes the large stress, partially. PSZ is known as a type of ceramics similar to metallic material. However, internal stress remained in this case around the grain boundary due to its large particle size, in spite of utilizing martensite transformation. Frequently, ceramics consists of different crystals. Therefore, the residual stress is generated in the cooling process after sintering, due to the different thermal expansion coefficients of matrix and crystal.

The large width of the grain boundary, in which inter-granular fracture is predominant, brought about a large crack opening displacement. The bad wetting between crystals or between crystal and matrix also causes the inter-granular fracture. These factors concern the microstructure, and the effect of the cyclic fatigue behavior, mechanically or thermally. Therefore, the developing fracture toughness of ceramics, fatigue life is inclined to shift the short life side. K_I-V curve for poly-crystal shift to the large K_I side but exhibit inferior mechanical properties, compared with that for single crystal. Evaluation techniques must be established for many mechanical properties, taking into account the incompatible properties of ceramics.

CONCLUSION

Mechanical and thermal fatigue test were carried out for alumina ceramics and the following results were obtained.

1) The difference of fundamental properties with fracture mechanics was related to the fracture behavior, in which the inter-granular fracture was predominant.

2) R-curve appeared with increasing particle size for alumina ceramics, but acceleration to the short life time was observed on cyclic fatigue test.

3) The connection of cusp in grain boundary may accelerate the crack propagation on the cyclic fatigue test.

4) As the stress ratio could not changed for the thermal fatigue test, the fatigue parameter n hardly changed. However, the fatigue parameter A changed clearly in correspondence with the microstructure.

5) The n values on thermal fatigue test were nearly equal to those on mechanical fatigue test.

REFERENCES

1) H. Kamiya, M. Takatsu, K. Ohya, M. Ando, A. Hattori, "Effect of Microstructure on Cyclic Fatigue Properties of Al_2O_3 Ceramics and Al_2O_3 Composites" J. Ceram. Soc., Japan, 98, 456-63(1990).

2) T. Nishikawa, T. Gao, T. Nishibe, M. Takatsu, "Thermal Fatigue Behavior of Alumina Ceramics by Water Quencing Method" The Ceramic Society of Japan 1991 Annual Proceedings, 576(1991).

3) M. Takatsu, H. Kamiya, K. Ohya, K. Ogura, T. Kinoshita, "Effect on Vibrated Cyclic Fatigue Properties of Ceramics from Stress Load Condition" J. Ceram. Soc., Japan, 96, 990-96(1988).

4) M. Takatsu, J. Takahashi, T. Nishikawa, K. Ohya, A. Hattori, "Cyclic Fatigue Properties of Piezoelectric Ceramics" ibid.,98, 1343-48(1990).

5) W.P.Minner, R.C.Bradt, "(K-V) Diagrams for Ceramic Materials" J. Am. Ceram. Soc., 58, 345-46(1975).

6) H. Kobayashi, T. Kawakubo, "Fatigue-Difference between Ceramics and Metal-" J. of the Japan Institute of Metals, 27, 757-65(1988).

7) N. Kamiya, O. Kamigaito, "Prediction of Thermal Fatigue Life of Ceramics" J. Material Soc., 14, 573-82(1979).

8) Y. Mizutani, M. Takatsu, K. Tamai, "New Introducing Method of Fatigue-crack " The Ceramic Society of Japan 1989 Annual Proceedings, Tokai Branch, (1989).

9) R.O. Richie, R.H. Dauskardt, W. Yu, A.M. Brendzel, "Cyclic Fatigue-crack Propagation, Stress-corrosion, and Fracture-toughness Behavior in Pyrolytic Carbon-coated Graphite for Prosthetic Heart Valve Applications" J. Biomed. Mater. Res., 24, 189-206(1990).